Received: 14 August 2023 | Revised: 22 January 2024 | Accepted: 1 February 2024

DOI: 10.1002/mawe.202300093

ARTICLE

WILEY VCH

Electrochemical hydrogen permeation measurement during cyclic stress testing of a ferritic chromium steel

Elektrochemische Messung der Wasserstoffpermeation während einer mechanischen Wechselbelastung für einen ferritischen Chromstahl

J. M. Vatter | B. Jung | M. Oechsner

Zentrum für Konstruktionswerkstoffe, Technische Universität Darmstadt, Darmstadt, Germany

Correspondence
J. M. Vatter, Zentrum für Konstruktionswerkstoffe, Technische Universität Darmstadt, Grafenstraße 2, 64283 Darmstadt, Germany.
Email: jannik.vatter@tu-darmstadt.de

Funding information
DFG, Grant/Award Number: ME 3301/4-1 | OE 558/13-1

Abstract

In the present work, the hydrogen diffusion during cyclic stress testing in the ferritic chromium steel 1.4521 (X2CrMoTi18-2) is investigated. Therefore, electrochemical hydrogen permeation measurements are carried out on a hollow cylinder geometry. Simultaneously an alternating stress is applied using a stress ratio of R = -1. At low stress amplitudes, no influence on the diffusion behaviour of hydrogen is found. At a higher stress amplitude, close to the macroscopic yield strength, a delayed hydrogen permeation by a factor of two is observed. It is postulated that this observation is a result of the nucleation of new hydrogen traps during the measurement. Hydrogen content measurements using carrier gas hot extraction support this hypothesis.

KEYWORDS
electrochemical, ferritic chromium steel, hydrogen, permeation

SCHLÜSSELWÖRTER
elektrochemisch, ferritischer Chromstahl, Permeation, Wasserstoff

1 | INTRODUCTION

While some experts assume that different concepts will have to exist simultaneously in the future, it is discussed that battery-based technologies and natural gas as an energy carrier as well as fuel are only preliminary stages of a hydrogen based economy [1, 2]. Just recently, Airbus presented three concepts that are intended to implement the first hydrogen-based air traffic by 2035. But not only the transport sector, also the energy sector, metal industry and pharmacy argue about the adaptation of hydrogen as gaseous energy carrier as a substitution to oil and gas [3]. Thus, the integrity of the currently existing infrastructure for the future transport and storage of an increased amount of hydrogen must be verified and possibly redesigned.

Hydrogen, compared to other gas species, can easily diffuse into and through metallic components. This not only makes the storage of hydrogen more difficult, but also may cause, as is well known, changes in the material properties. It could conduct hydrogen embrittlement, as a result of which a component fails prematurely. The

subject has been discussed in literature for decades and there are various hypotheses that describe a possible mechanism of damage [4, 5].

The presence of hydrogen is of decisive importance for the damage mechanism and thus also the diffusion of the same, as well as a possible acceleration under simultaneous mechanical stress. According to the Gorsky effect, lattice expansions due to a stress gradient represent a diffusion driving force and an acceleration of diffusion could be discussed [6]. Another transport-accelerating influence could act as a result of the increased dislocation velocity caused by the hydrogen-enhanced localized plasticity mechanism [7]. It is conceivable that, after the onset of plastic deformation, the transport of hydrogen is accelerated if it moves along with the dislocation [8, 9].

The two phenomena mentioned above (Gorsky effect and enhanced dislocation movement) are confronted by a number of studies that document a delay in hydrogen permeation by simultaneously applied mechanical stress [10–12]. While no influence of the stress on the hydrogen permeation was observed in the elastic stress range, the diffusion rate seems to decrease when a plastic deformation is initiated. The authors cite the dislocation density, which increases as a result of plastic deformation and which acts as a so called hydrogen trap [10]. Other studies investigating the effect of hydrogen traps on hydrogen permeation with regard to three different heat treatments came to the conclusion, that the measured delay cannot solely be explained by dislocation density [13]. The measured dislocation density did not correlate with the observed relative decrease in effective diffusivity. A higher energetic trap is necessary to cause the observed delay. For the three heat treatments investigated it was postulated to be most likely retained austenite and grain boundaries.

The mentioned articles are based on experiments carried out on constant stress levels and/or different microstructural configurations. In the present work we will address the change in hydrogen permeation caused by an simultaneous alternating mechanical stress application.

2 | MATERIAL AND SAMPLING

For the investigations a ferritic chromium steel 1.4521 (X2CrMoTi18-2) was used, Tables 1, 2. As sample geometry a hollow cylinder was used to simulate a tube or pipe, Figure 1. The inner and outer diameter was set to 13 mm and 15 mm respectively, resulting in a wall thickness of 1 mm.

3 | EXPERIMENTAL

The measurement of hydrogen permeation is based on the electrochemical concept of Devanathan and Stachursky, which is also used in DIN EN ISO 17081 [14, 15]. The experimental setup is adopted to the sample geometry, Figure 1. Inside the cylindrical hollow sample (reduction chamber), a constant supply of hydrogen is provided on the inner surface via cathodic polarization through the electrolysis of water. Polarization was regulated at $-5\ \frac{mA}{cm^2}$ in a 0.1 M sodium hydroxide solution. A platinum wire runs through the hollow sample and is conducted as counter electrode. The silver/silver chloride reference electrode is connected via a salt bridge. The oxidation current is measured on the outside of the sample. For this purpose, the sample is anodically polarized in 0.1 M sodium hydroxide against a second silver/silver chloride reference electrode to $+540\ mV_{SHE}$ ($+339\ mV_{Ag/AgCl}$ against the used reference electrode). As a counter electrode a platinum mesh is shaped around the sample. Experiments were run without the application of a palladium coating for the sample. Due to the high chromium content in the examined material, it can naturally form a sufficient passive layer which protect the base material of anodic dissolution. This passivation first results in a measured current signal and is taken

TABLE 1 Measured chemical composition of the used material 1.4521 (X2CrMoTi18–2) in wt%.

C	Si	Mn	P	Cr	Mo	Ni	Ti
0.011	0.753	0.231	0.015	20.39	1.97	0.071	<0.01
± 0.002	± 0.052	± 0.023	± 0.002	± 0.1	± 0.03	± 0.001	

TABLE 2 Measured mechanical properties of the used material 1.4521 (X2CrMoTi18–2).

Material	Proof stress $R_{p0.2}$ [MPa]	Tensile strength R_m [MPa]	Fracture elongation A [%]	Reduction of area Z [%]
1.4521	372 ± 1	523 ± 4	34.8 ± 0.2	80 ± 0.8

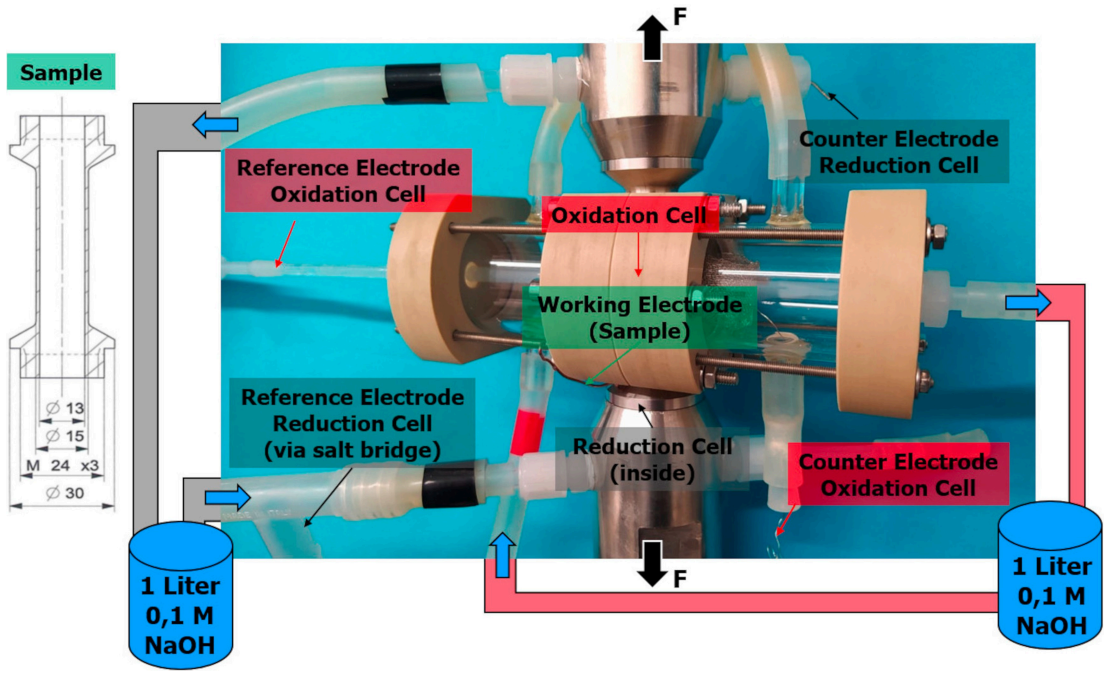

FIGURE 1 Experimental setup for the electrochemical permeation measurement during cyclic mechanical stress testing.

into account as such in the later evaluation of the permeation signal. The overall test duration (accumulated time) results of a compromise between the number of cycles, which may not lead to crack initiation, and the time necessary to measure hydrogen permeation, Table 3. The same applies for the load frequency which is 1 Hz for a stress amplitude of $\sigma_{a,n} = 100\ MPa$and 0.01 Hz for $\sigma_{a,n} = 300\ MPa$and above. Stress ratio is set to R =-1. Parameters were chosen conservatively on the basis of S/N curves carried out for the same material in pressurized hydrogen at 50 bar published elsewhere [16].

The test period begins with the filling of both chambers with the electrolyte, the start of the anodic polarization in the oxidation chamber and the start of the mechanical load. First, the current resulting due to the passivation of the sample is measured in the oxidation chamber for 24 h. The first hydrogen charging then starts on the inner surface of the hollow sample (reduction chamber). After the first hydrogen charging, the sample is discharged for 37 h before the second charging begins. The transient of the second charging is the one evaluated later. Reason of the repeated charging is to saturate the existing irreversible hydrogen traps inside the sample so that the second transient is not influenced by these anymore [15, 17].

In literature we find a diffusion equation with an analytical solution for hollow cylinders in accordance with the boundary conditions also presented here [18, 19]. Diffusion according to Fick is assumed with the diffusion coefficient being constant (independent of the concentration). For a diffusion from the inside to the

TABLE 3 Experimental matrix for the electrochemical hydrogen permeation measurement during cyclic mechanical stress testing at a stress ratio $R = -1$.

Sample number	1	2	3	4	5	6
Stress amplitude [MPa]	0	100	300	350	300	300
Frequence [Hz]	–	1	0.01	0.01	0.01	0.01
Number of cycles [−]	–	324000	3240	3240	4932	4932
Accumulated time [h]	89	89	89	89	137	137
Passivation time [h]	24	24	24	24	24	24
1. Hydrogen charging [h]	14	14	14	14	38	38
Discharging [h]	37	37	37	37	37	37
2. Hydrogen charging [h]	14	14	14	14	38	38

outside, equation (1) results with the boundary conditions according to equations (2) and 3.

$$\frac{J^b(t)}{J^b_\infty} = 1 - \pi k l n(k) \sum_{n=1}^{\infty} \frac{a\alpha_n J_0^2(ka\alpha_n)\left[\begin{matrix} J_0(a\alpha_n)Y_1(ka\alpha_n) - \\ Y_0(a\alpha_n)J_1(ka\alpha_n) \end{matrix}\right]}{J_0^2(a\alpha_n) - J_0^2(ka\alpha_n)} * \exp\left[-(a\alpha_n)^2 \frac{D_{eff} t}{a^2}\right] \quad (1)$$

$$k = \frac{b}{a} \quad (2)$$

$$J_0(a\alpha_n)Y_0(b\alpha_n) - Y_0(a\alpha_n)J_0(b\alpha_n) = 0 \quad (3)$$

With $a = inner\ radius$, $b = outer\ radius$, $J_\nu(X) = Bessel\ function\ 1st\ kind\ of\ order\ \nu$ and $Y_\nu(X) = Bessel\ function\ 2nd\ kind\ of\ order\ \nu$ are being defined by the sample geometry. $t = time$ being the independent variable. The effective diffusion coefficient D_{eff} is to be constant. $J^b(t)$ is the time dependent evolution of the particle flow through the outside of the sample, in our case hydrogen atoms and J^b_∞ is the particle flow through the outside of the sample after reaching steady state for $t \to \infty$. Finally, α_n are the positive roots of Eq. (3), Table 4. Thus, for n = 1, 2, 3, 4, 5, the time-lag results according to equation 4.

$$T_{lag,sample} = \frac{0.17\ mm^2}{D_{eff}} \quad (4)$$

The time-lag method is commonly used for evaluation of permeation measurements and can be looked up in various literature [20].

For this specific geometry the deviation compared to a flat sample is comparatively small, equation (5) [15, 20].

$$T_{lag,\ flat} = \frac{L^2}{6D_{eff}} = \frac{1\ mm^2}{6D_{eff}} \quad (5)$$

The effect of sample geometry will become more significant with increasing $k = \frac{b}{a}$, [19].

Hydrogen content measurement using carrier gas hot extraction was carried out after the permeation treatment on the same samples. Prior to the measurement, the samples were once again electrochemically charged with hydrogen for 48 h and then discharged for 48 h without any applied stress. The thereafter residual hydrogen content of the samples was driven out in a preheated infrared light tube at 900 °C. After introducing the samples into the infrared tube, the effusing hydrogen was recorded for 1 h.

TABLE 4 Calculated positive roots for $J_0(a\alpha_n)Y_0(b\alpha_n) - Y_0(a\alpha_n)J_0(b\alpha_n) = 0$.

k	$a\alpha_1$	$a\alpha_2$	$a\alpha_3$	$a\alpha_4$	$a\alpha_5$
1.15	20.42	40.84	61.26	81.68	102.1

4 | RESULTS

According to the described experimental setup and equation (1) an effective hydrogen diffusion coefficient is measured rather than the lattice diffusion coefficient. To determine the effective hydrogen diffusion coefficients D_{eff}, the second transient of two sequential hydrogen permeation measurements was used, Figure 2. D_{eff} was calculated analytical using the time-lag method as well as numerical by fitting equation (1). Results of both ways are comparable but the measured transient is steeper than the fitted one, Figure 3. A comparison of the effective diffusion coefficients, which were determined for an experiment with a cyclic stress amplitude of $\sigma_{a,n} = 100\ MPa$ deviate just slightly from the coefficients which were determined in a zero-stress condition. Thus, for this stress level, there is no influence of the stress amplitude on the diffusion behavior of the material. For measurements with higher stress amplitudes of $\sigma_{a,n} = 300\ MPa$ and $\sigma_{a,n} = 350\ MPa$ respectively, no hydrogen permeation transient could be detected on the outside of the sample in the period of a 14 h charging, sample 3 and 4 in Table 3. The macroscopic yield

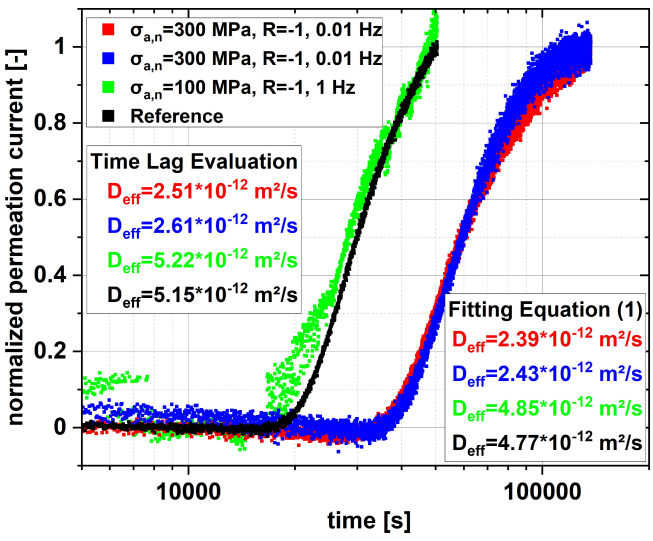

FIGURE 2 Electrochemical permeation measurement and thereafter calculated diffusion coefficient D_{eff} for different applied stress levels.

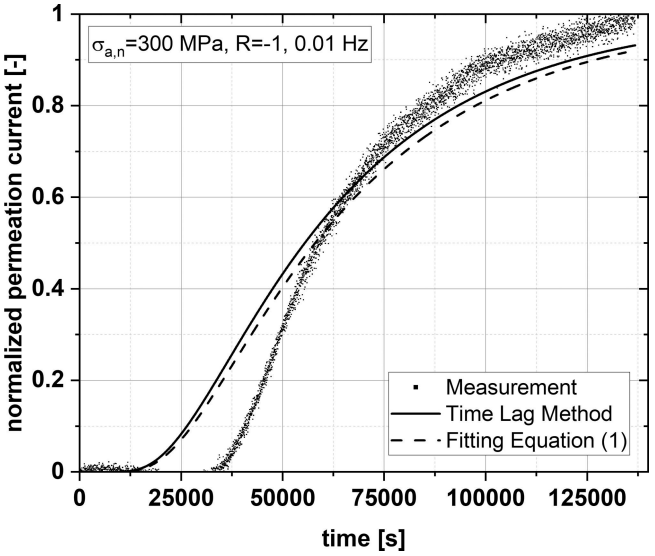

FIGURE 3 Comparison of the as measured permeation transient to the ideal transient according to equation (1).

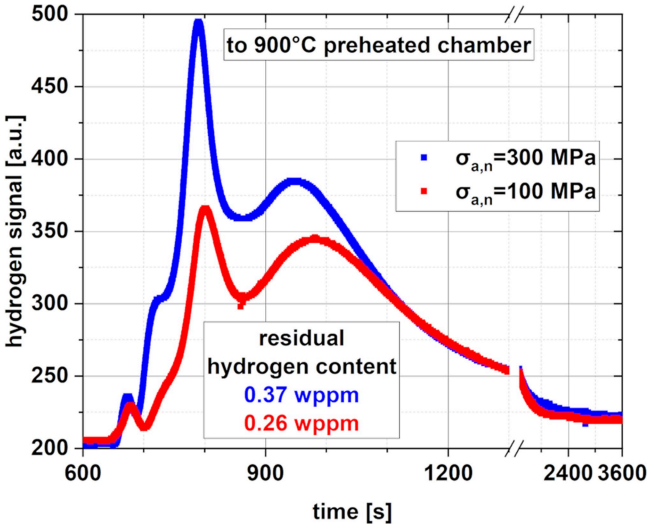

FIGURE 4 stress amplitudes of $\sigma_{a,n} = 300$ MPa and $\sigma_{a,n} = 100$ MPa respectively. Additionally, the samples were electrochemicaly charged and discharged once again before measurement for 48 h + 48 h.

strength for the material is about $R_e = 320\ MPa$. A transient only occurred while already discharging in preparation for the second charging, meaning that the hydrogen permeation was delayed in time. In further experiments, the charging times therefore were adjusted to 38 h, sample 5 and 6. An evaluation of the permeation transients then led to a calculated effective diffusion coefficient which is lower by a factor of two compared to the reference without any applied mechanical stress.

In addition to the hydrogen permeation measurements, the residual hydrogen content in the samples, which were tested with a cyclic stress amplitude of $\sigma_{a,n} = 100\ MPa$ and $\sigma_{a,n} = 300\ MPa$, was measured using carier gas hot extraction, Figure 4. Both Samples indicate a superposition of four individual peaks with similar profile. Therefore, the heating and effusion behavior of the samples seems to be comparable. However, the hydrogen content, determined by the integral of the hydrogen signal measured, is with 0.37 wppm around 50% higher in the sample tested with a stress amplitude of $\sigma_{a,\,n} = 300\ MPa$ compared to the 0.26 wppm of the sample tested at $\sigma_{a,n} = 100\ MPa$.

5 | DISCUSSION

The lattice diffusion coefficient of hydrogen in low carbon steel at room temperature is of about $D = 7.2^{*}10^{-9}\ \frac{m^2}{s}$ [21]. Due to the interaction of hydrogen with trap sites such as voids, precipitates, dislocations, grain boundaries, etc. the effective diffusion coefficient is lower and varies depending on cold forming and heat treatment. Values varying between $D_{eff} = 1.4^{*}10^{-10}\ \frac{m^2}{s}$ and $D_{eff} = 3.5^{*}10^{-11}\ \frac{m^2}{s}$ are stated for pure iron [17,22].

The effect of trap sites on hydrogen permeation and the effective diffusion coefficient largely depends on the trap density and the binding energy [21, 23]. Strictly speaking the effective diffusion coefficient decreases with increasing trap density as well as increasing binding energy. A higher trap density reduces the hydrogen flow as long as there are trap sites that can be occupied. Only once the traps are fully occupied does the effective diffusion coefficient approach the lattice diffusion coefficient [23]. The influence of the binding energy is related to the possibility of the hydrogen being released from a trap, i.e. detrapping. If the activation energy required for detrapping is higher, it will happen less frequently. The energy required for detrapping, E^d is the sum of the binding energy, ΔE and the activation energy for trapping, E^t with the binding energy accounting for the dominant share [21].

The effective diffusion coefficient measured in the experiments without mechanical stress is $D_{eff} = 5.15^{*}10^{-12}\ \frac{m^2}{s}$ and is therefore one order of magnitude lower than the values in literature for pure iron. This may be due to the alloying elements and the associated higher trap density. The fact that the second transient was evaluated indicates that in this case traps with higher binding energy, i.e. irreversible traps are responsible.

However, this might be different for the experiments carried out during cyclic stress application. Considering

the simultaneuos application of a cyclic stress, a change in microstructure during the time of permeation measurement, including the time beween the first and second transient, may be possible. Based on the calculated effective diffusion coefficient such a change is unlikely to happen for the stress amplitude of $\sigma_{a,n} = 100\ MPa$. The calculated two times lower effective diffusion coefficient for samples tested at a stress amplitude of $\sigma_{a,n} = 300\ MPa$ on the other hand allow the interpretation of microstructural changes during the permeation measurement. With respect to the macroscopic yield strength of $R_e = 320\ MPa$ of the material these plastic deformations consequently have to happen on a local microscopic scale. Samples were not loaded until fatigue therefore no fracture morphology was accessible for analysis.

This hypothesis is supported by the hydrogen content measurement carried out. The measured residual hydrogen content after an additional 48 h discharging refers to the at room temperature irreversibly bound hydrogen. A 50% higher content for the sample tested at $\sigma_{a,n} = 300\ MPa$indicate a higher trap density compared to $\sigma_{a,n} = 100\ MPa$. Although no activation energy for detrapping was measured, the similar characteristic of the four individual peaks in the hydrogen signal indicate a similar magnitude in this regard. It is therefore postulated that the measurements did not actually observe a lower diffusion coefficient in means of a lower jump rate (higher binding energy), but rather a delayed permeation caused by simultaneous new nucleated hydrogen traps of energetic similar magnitude as already present in the raw material. The investigated material does response with cyclic hardening both in air and in presurized hydrogen at 50 bar, as is published elswhere [16]. Therefore, the new hydrogen traps may origin from dislocations, slip-planes, disordered grains or their interactions.

6 | CONCLUSIONS

Electrochemical hydrogen permeation measurements during simultaneous application of an alternating mechanical stress with stress ratio R=-1 were carried out. Residual hydrogen content was measured using carrier gas hot extraction.

- At low stress amplitudes $\sigma_{a,n} = 100\ MPa$ no change in hydrogen permeation was observed and the diffusion coefficient was calculated to be $D_{eff} = 5.22^{*}10^{-12}\ \frac{m^2}{s}$
- Stress amplitudes of $\sigma_{a,n} = 300\ MPa$ that are close to the macroscopic yield strength $R_e = 320\ MPa$ result in a delayed hydrogen permeation by a factor of two
- Residual hydrogen content in a sample tested at $\sigma_{a,n} = 300\ MPa$ was 50% higher compared to $\sigma_{a,n} = 100\ MPa$ indicating a higher at room temperature irreversible trap density
- Similar characteristics in the hydrogen extraction profiles indicate, that the delay in hydrogen permeation for higher stress amplitudes may be caused by the nucleation of new traps instead of an actual decrease in the jump rate (binding energy) of hydrogen

CREDIT AUTHOR STATEMENT

J.M. Vatter: Methodology, Investigation, Formal Analysis, Writing – Original Draft, Visualization B. Jung: Supervision, Writing – Review & Editing M. Oechsner: Supervision

ACKNOWLEDGEMENTS

This article discusses results derived in the DFG research project “Grundlagen für die Bemessung druckwasserstoffexponierter Komponenten unter Berücksichtigung werkstoffspezifischer Eigenschaften und Schädigungsmechanismen“ (ME 3301/4-1 | OE 558/13-1).

Our thanks go to the German Research Foundation (DFG) for funding this project. Open Access funding enabled and organized by Projekt DEAL.

CONFLICT OF INTEREST STATEMENT

The authors declare no financial or commercial conflict of interest.

REFERENCES

1. European Commission, *Energy Roadmap 2050*, European Union 2012.
2. R. Appel, V. Kefer, *VDI Nachr.* **2021**, *75*.
3. Euroforum Deutschland GmbH, ed., *Energiewirtschaft: Dynamik Pur* 2021.
4. W. Gerberich, in Gaseous hydrogen embrittlement of materials in energy technologies, Volume 2: Mechanisms, modelling and future developments 2012, pp. 209–246.
5. S. Lynch, *Corros. Rev.* **2019**, *37*, 377.
6. J. Völkl, *Bunsenges. Phys. Chem.* **1972**, *76*, 797.
7. P. J. Ferreira, I. M. Robertson, H. K. Birnbaum, *Acta Mater.* **1998**, *46*, 1749.
8. A.-M. Brass, J. Chêne, *Corros. Sci.* **2006**, *48*, 481.
9. K. Takai, H. Shoda, *Rev. Mater.* **2010**, *15*, 267.
10. Y. Huang, A. Nakajima, A. Nishikata, T. Tsuru, *ISIJ Int.* **2003**, *43*, 548.
11. S. J. Kim, H. G. Jung, K. Y. Kim, *Electrochim. Acta* **2012**, *78*, 139.
12. D. Sun, M. Wu, F. Xie, K. Gong, *Int. J. Hydrogen Energy* **2019**, *44*, 24065.

13. A. Turk, G. R. Joshi, M. Gintalas, M. Callisti, P. E. J. Rivera-Díaz-del-Castillo, E. I. Galindo-Nava, *Acta Mater.* **2020**, *194*, 118.
14. M. A. V. Devanathan, Z. Stachurski, W. Beck, *J. Electrochem. Soc.* **1963**, *110*, 886.
15. DIN EN ISO 17081, DIN Deutsches Institut für Normung e. V., 2014–10, *ICS 77.060*.
16. S. Schoenborn, T. Melz, J. Baumgartner, C. Bleicher, *Procedia Struct. Integr.* **2021**, *33*, 757.
17. T. Zauchner, *Diplomarbeit*, Montanuniversität Leoben, 2015.
18. H. S. Carslaw, J. C. Jaeger, *Conduction of heat in solids*, Oxford: Clarendon Press 1959.
19. I. B. Huang, S. K. Yen, *Mater. Chem. Phys.* **2002**, *74*, 289.
20. J. Crank, *The Mathematics of Diffusion*, Oxford : Clarendon Press 1975.
21. A. Turnbull, R. B. Hutchings, D. H. Ferriss, *Mater. Sci. Eng. A* **1997**, *238*, 317.
22. H. Addach, P. Berçot, M. Rezrazi, J. Takadoum, *Corros. Sci.* **2009**, *51*, 263.
23. A. Turnbull, *Int. J. Hydrogen Energy* **2015**, *40*, 16961.

How to cite this article: J. M. Vatter, B. Jung, M. Oechsner, *Materialwiss. Werkstofftech.* **2024**, *55*, e202300093. https://doi.org/10.1002/mawe.202300093